

An infectious diseases hazard map for India based on mobility and transportation networks

Onkar Sadekar, Mansi Budamagunta, G. J. Sreejith, Sachin Jain, and M. S. Santhanam

Indian Institute of Science Education and Research, Pune 411 008, India.

December 30, 2021

Abstract

We propose and construct an infectious diseases hazard map for India. Given the outbreak location for infectious disease, hazard map quantifies the infection risk faced by cities and towns in India. A framework consisting of a SIR metapopulation model augmented with mobility data is used to simulate the spread of infectious diseases. Despite multiple India-focused studies on this topic, very few focus on long-distance travel as the dominant mode of infection spread. Using extensive real data and estimates of air, rail, and road mobilities, a transportation and mobility network of 446 Indian cities having a population higher than 1 Lakh is constructed. Based on a notion of an *effective distance* that incorporates mobility information, a hazard value is assigned to each city for a given outbreak location. It is shown that the effective distance, rather than the geographical distance, from the outbreak location has a linear relation with the time of arrival of infection at every city, and hence provides a better measure of risk. The estimated hazard index is also compared with real data of SARS-CoV-2 spread during the first wave in 2020 and a good agreement is seen. With better mobility data, the proposed hazard map framework can be used for any other infectious disease spread in the future.

1 Introduction

As of December 30, 2021, more than 15 Crore (150 million) people have been infected by the SARS-CoV-2 strain, and about 32 Lakh (3.2 million) have deceased [1], since it was first reported from Wuhan in China in December 2019. SARS-CoV-2 has infected almost one in every 50 people in the world. With the resurgent second wave becoming more virulent in India since March 2021, the number of infections and deaths have witnessed a steep increase [2]. Thus, starting with just about a cluster of cases reported in Wuhan, it has emerged as one of the unprecedented global public health crisis. In India, starting with just a couple of cases in February 2020, the infections had spread to about 65 Lakh people by September 2020, in just a span of about eight months. It is well appreciated that irrespective of the virus' innate

capacity to cause disease and even deaths, the spread from one geographical area to another is primarily caused by the mobility of the people [3, 4, 5, 6].

The Spanish Flu of 1918 was one of the biggest pandemics to hit India in the early 20th century, arriving in Bombay through the British-Indian army returning after the end of the first world war in Europe [7]. The annual report of the Sanitary Commissioner to the Government of India in 1918 observed that “There is ample evidence during the first epidemic of the introduction of infection into a locality from another infected locality. The railway played a prominent part, as was inevitable. During the panic caused by the epidemic, the trains were filled with emigrants from infected centres, many of them being ill. The Post office also was an important agency in disseminating infection, also very largely through the Railway Postal Service. Lucknow, Lahore, Simla and other cities are said to have been infected in this manner” [8]. Further, the report states that “there is ample evidence to prove that infection in India during the second epidemic was carried from province to province and place to place within each province by travellers by rail, riverboats, carts and on foot”. This mode of spread has also been confirmed by other studies based on the detailed data recorded then in Bombay and other provinces of British India [7]. Nearly one century after the Spanish Flu, the advancements in technology have led to faster and efficient modes of transportation, and the world has become “smaller” than ever before. Long-distance travel is not considered to be either dangerous or luxury anymore. However, as shown in many studies in the past decade, it has also helped the spread of infectious diseases to remote corners of the world on short time scales [9, 10, 11].

Independent of the severity of the infection and its place of an outbreak, the various transportation modes serve to spread them far and wide. This is evident in the spread of SARS-CoV-2 in India, as was the case with other infectious diseases reported globally earlier [12, 13, 14, 15]. While much of the modelling efforts were directed towards predicting the evolution of caseloads in cities and towns across India [16, 17, 18, 19, 20, 21], it is also imperative to understand the macroscopic spreading pattern of infectious diseases. Thus, in the context of SARS-CoV-2 spread in a large country, generally, one might identify two concurrent but distinct processes – (a) the evolution of infection caseloads within a small geographical boundary such as a city or a town, and (b) the transmission of infection from one geographical area to another, *i.e.*, from, say, one city to another. The latter process will depend crucially on the transport networks and the mobility patterns of people within the country [22, 23, 24, 25]. The trivial and rather impractical limit is when transportation systems are entirely stopped leading to infection dying down in its outbreak location. Given the growth pattern of SARS-CoV-2 infection in India, it is only natural to discuss how transportation networks can provide quantitative information about the spread of infection.

In this work, we propose and estimate an infectious diseases hazard map for India, somewhat similar to the seismic hazard maps produced for earthquakes [26]. By employing the transportation networks and the consequent mobility patterns, the spread of infection can be estimated starting from its declared outbreak location. For instance, in the case of SARS-CoV-2, though first official cases were detected

from international passengers arriving in Kerala, by early April 2020, a significant outbreak (implying several 100s of infection cases) was reported from Mumbai, and Delhi [2]. As these cities represent large transport hubs in India, the infection spread into other parts of the country very soon. Hence, it would seem natural to define a hazard index for every city and town in India, which will be obtained based on the connectivity matrix and mobility volumes. The question can be posed as follows – in a network of N cities/towns given by $X_1, X_2, X_3, \dots, X_N$, and if the infection outbreak location is declared to be X_1 , can a hazard value be assigned to other cities/towns X_2, \dots, X_N reflecting, not their geographical proximity to X_1 , but their ability to catch the infection due to an “effective proximity” incorporating mobility patterns? We discuss one solution to this question, extensively using modelling and data from India’s air, railway and road transportation networks and mobility patterns.

It must be emphasised that the proposed hazard index (on which the hazard map is based) depends both on the outbreak location and the mobility patterns, the latter, in general, is a time-dependent factor. Thus, the hazard index could, in general, be time-dependent. However, considering that the volume of infection cases does not change appreciably in timescales of less than a day, and in any case, the data is made public only on a granularity of a day, we construct the hazard map for India in this paper by assuming averaged mobility (averaged over few days) to be representative for all times. For a hazard map at a subcontinental spatial scale such as India, the mobility patterns within a city or town or even within districts are ignored. Incidentally, some aspects of the local mobility are captured by the Google mobility data and are useful for planning at the district or even municipal level, but they are not considered here. In this work, the mobility data and model are applied to obtain a hazard map for cities and towns with a population of more than one Lakh, *i.e.*, 446 of them [27].

The plan for this paper is as follows. In the next section (2), we discuss the SIR-model augmented with mobility of people between the cities via air, trains and roads. In section (3), the data sources and their details, such as its properties and how it compares with known data sources are discussed. A hazard index is defined in section (4) for a given outbreak location. In section (5), the main results are given. Finally, the results are compared with real-life conditions at a coarse level. Finally, section (6) concludes with a brief summary.

2 Augmented SIR model framework

The overall model framework is based on the susceptible-infected-recovered (SIR) compartmental model augmented with connectivity information between towns and cities [12, 28].

For a well-mixed population, the standard SIR-compartmental model [29, 30] is given by the set of three coupled differential equations :

$$\begin{aligned}\frac{\partial S(t)}{\partial t} &= -\alpha \frac{S(t)I(t)}{N}, \\ \frac{\partial I(t)}{\partial t} &= +\alpha \frac{S(t)I(t)}{N} - \beta I(t),\end{aligned}$$

$$\frac{\partial R(t)}{\partial t} = +\beta I(t). \quad (1)$$

In this, $S(t)$, $I(t)$ and $R(t)$ denote the susceptible, infected, and recovered population respectively at time t , α denotes the per capita rate of infection, and β is the recovery rate. If N is the total population, then $N = S(t) + I(t) + R(t)$ remains constant in time. However, in reality, the population in India (or, for that matter elsewhere) is not well-mixed, for reasons of variations in traffic patterns between cities to non-uniform population density. Thus, a network of M cities/towns is considered. It is assumed that the population within each city/town is reasonably well-mixed and Eqs. (1) would apply. A small proportion of this population can travel between different cities/towns, according to the following equation for movement kinetics,

$$\frac{\partial N_n(t)}{\partial t} = \sum_{m=1}^M \left[W_m^n N_m(t) - W_n^m N_n(t) \right], \quad n, m = 1, 2, \dots, M, \quad (2)$$

where $N_i(t)$ denotes the population of i -th city/town at time t , W_i^j denotes the rate of people leaving city i and going to city j . In other words, $p(j, t + \Delta t | i, t) = W_i^j \Delta t$, such that $p(j, t + \Delta t | i, t)$ denotes the conditional probability that an individual in city i at time t , would be in city j at time $t + \Delta t$. Mobility is incorporated through the traffic matrix \mathbf{F} , such that the element F_i^j denotes the number of people going from city i to j per unit time. There are no self loops in the network and hence $F_i^i = 0$. Thus, $F_i = \sum_j F_i^j$ denotes the total number of people leaving city i per unit time. Now, the probability that an individual travels from city i to j is simply $W_i^j = F_i^j / F_i$. Substituting this in Eq. (2), we obtain

$$\frac{\partial N_n(t)}{\partial t} = \sum_m [F_m^n - F_n^m] \quad (3)$$

Physically, it is clear that if the influx to a city and outflux from it is equal, then the city's total population $N_n(t)$ will be a constant. This can be inferred from Eq. (3) by summing over m . Then, the right-hand side will become $F^n - F_n$, representing the influx and outflux terms respectively for city n . If outflux is equal to the influx, then $F^n - F_n = 0$ and thus $N_n(t) = N_n$, a constant. In the rest of the manuscript, the population of each city is taken to be constant with time. The time scale in which the infection typically spreads is much smaller than the time scales in which the population of the city increases. Population in a city could increase either due to immigration or enhanced birth rates. The time scales over which these processes happen is far longer than the infection spreading timescale. Even within these constraints, generally $F_i^j \neq F_j^i$, *i.e.*, the flux of passengers from one city to another is not an equilibrium process, and detailed balance is not satisfied. We will infer the same conclusion from the flux data as well.

In order to integrate the movement kinetics into the SIR model, it is assumed that the probability of getting infected during the transit is zero. There is not much of reliable data about infection acquired during transit, and in any case, it is likely that its contribution to the infection case load is sufficiently small and can be safely neglected. In our modelling context, if a person is susceptible when leaving city i , he/she would remain so when he/she reaches city j , and similar is the case for infected or recovered

persons. Then, under these assumptions, the SIR model in Eqs. (1) incorporating the flux of people between M cities, can be written down as

$$\begin{aligned}\frac{\partial S_n(t)}{\partial t} &= -\alpha \frac{S_n(t)I_n(t)}{N_n} + \sum_m \left[\frac{F_m^n}{N_m} S_m(t) - \frac{F_n^m}{N_n} S_n(t) \right], \\ \frac{\partial I_n(t)}{\partial t} &= +\alpha \frac{S_n(t)I_n(t)}{N_n} - \beta I_n(t) + \sum_m \left[\frac{F_m^n}{N_m} I_m(t) - \frac{F_n^m}{N_n} I_n(t) \right], \\ \frac{\partial R_n(t)}{\partial t} &= +\beta I_n(t) + \sum_m \left[\frac{F_m^n}{N_m} R_m(t) - \frac{F_n^m}{N_n} R_n(t) \right], \quad n, m = 1, 2, \dots, M.\end{aligned}\tag{4}$$

It can be verified, by adding the three equations, that $S_n(t) + I_n(t) + R_n(t) = N_n$ is a constant, upto small deviations arising on account of F_i not being strictly equal to F^i ; which we can ignore for the short time scales considered in this work. In the rest of the paper, Eqs. (4) will be the central framework supplemented with India specific data to estimate traffic matrix \mathbf{F} . As we shall see, estimating \mathbf{F} is easier said than done and depends on the availability of mobility data.

It might be emphasised that at this point, Eqs. (4) are quite general and are not India-specific. It can be applied for other countries as well, or even on a global scale, [12, 31]. The SIR-type compartmental model is useful for predicting infection growth in a *well-mixed* population. Thus, Eqs. (4) can be thought of as an extension of the SIR model to a network of cities/towns, especially in the case of populations not being well mixed. In particular, this equation incorporates large flux between the cities/towns in the network. The former scenario has been well studied in the literature, though incorporation of the flux of people between cities/towns has not been studied sufficiently well [32, 33].

3 Transportation network and data

From this point onwards, our discussion will be India specific. In this section, network creation and data sources used in estimating the traffic matrix \mathbf{F} are discussed. Though people in India use many forms of transport, for the purposes of this work, we focus on data from air, railway and road transportation while ignoring inland waterways and other modes.

Based on the census data of 2011 [27], a network of cities/towns in India whose population is more than 1 Lakh is created. It is also ensured that these towns and cities have at least one of air, rail or road connectivity. By this criterion, a directed network that has $M = 446$ nodes (cities/towns), and 46448 edges (routes) is created. In this, the edges corresponding to air, railway and road links are combined if they connect the same pair of cities and are counted as one edge. Some of the important network properties are listed in Table (1). In the table, mean degree refers to the out-degree (which is the same as in-degree for this dataset) and gives a measure of the average number of cities each city is connected to. This table also shows coarse mobility data. By ‘route symmetry index’ in the context of pair of cities a and b , it is indicated if route $a \rightarrow b$ has the same traffic as the reverse route $b \rightarrow a$ or not. The index is defined for a given dataset as ‘1– the maximum absolute fractional traffic difference with respect to

the city’s population averaged over all cities’. The index can mathematically be expressed as

$$\text{Route Symmetry Index} = 1 - \left\langle \frac{\max_j \{|F_i^j - F_j^i|\}}{N_i} \right\rangle_i. \quad (5)$$

The locality of mobility indicates if the fraction of people who travel out of a city, i.e. $\frac{F_i}{N_i}$, is the same across all cities or not. As is evident, air travel contributes far less to the overall mobility of people in India though it might become somewhat important if the speed of transportation is taken into account. As road travel is a locally (< 300 km) dominant mode, most of the meaningful long-distance connections and mobility arise from railways.

| Property | Airway | Railway | Roadway | Combined |
|----------------------|-------------------|-------------------|-------------------|-------------------|
| Number of Nodes | 85 | 435 | 446 | 446 |
| Number of Edges | 1182 | 41594 | 9128 | 46448 |
| Average Degree | 13 | 95 | 20 | 104 |
| Route symmetry index | 1 | 0.9875 | 1 | 0.9878 |
| Locality of Mobility | Same | Different | Same | Different |
| Passengers/day | 7.5×10^5 | 8.8×10^6 | 2.5×10^6 | 1.2×10^7 |
| Fraction of total | 0.06 | 0.73 | 0.21 | 1.0 |

Table 1: Properties of the transportation network and mobility data assembled for this work. Not surprisingly, air travel constitutes a miniscule fraction of the overall mobility. Bulk of long distance travel is accounted for by trains, though at short distances roads might also have significant contribution.

Railway data : The data of trains and railway stations was obtained from the Indian Railways website, and private travel planning websites [34, 35]. In all, Indian railways has about 8000 railway stations on its network, and about 3000 express/mail/passenger trains are run on this network [36]. The weekly schedule of each of these trains is drawn from the railway timetable [36]. Even though there are studies conducted to analyse the Indian railway network [37, 38, 39], none of them considered the number of passengers travelling between two cities. The data of the number of trains run is converted into passenger traffic through an algorithm described in the Supplemental material [40]. The algorithm relies on two simple assumptions – that the train is always full (almost always true in India), and the number of passengers travelling between two cities on some route is proportional to the population of the two cities. Based on this algorithm, the daily passengers on the train comes to about 88 Lakh [Table

(1)]. As we are only concerned with long-distance traffic, the suburban traffic in several cities such as Mumbai and Chennai, which have a dense suburban train network, is also ignored. As per the Indian Railway’s facts and figures, [41], the non-suburban passengers were 355 Crores in 2016-17, which gives daily non-suburban traffic of around 97 Lakh passengers per day. Thus, our estimate differs by about 9% from the official data. However, that can be attributed to incomplete information about all train routes on the Indian railway’s website and ignoring all the smaller stations in the country. Additionally, we have assumed that the train is always full to its capacity. However, we are well aware from daily experience that trains often exceed their capacity on many routes.

Airline data : The passenger data on domestic routes, based on the data available on the Directorate General of Civil Aviation, Govt. of India (DGCA), was obtained [42] for 85 Indian cities with an airport and with a population of 1 Lakh or more. Passenger traffic was collected for pairs of cities for the year 2018, from which daily traffic was arrived at. According to the DGCA, the total domestic air traffic in India for 2018-2019 was 2851 Lakhs [43]. This implies that about 7.8 Lakhs people use air transport daily on an average, which upon correcting for the ignored airports for small cities with a population less than 1 Lakh, comes to approximately 7.5 Lakhs per day, the value indicated in Table (1).

Road data : Compared to the other two modes of transport, very little reliable information is available for road transport in India. The National Highways Authority of India (NHAI) provides some minimal data only for national highways, which typically carry traffic over long-distances of >300-400 Kms. However, we ignore the long-distance road traffic by assuming that people mostly prefer train or air for long-distance travel. Further, the significant passenger flux over short distances of about <400 km is mainly accounted for by public transport and in some cases by private vehicles. Since there is no reliable data available to estimate the short distance (<400 Kms) travel (or even the long-distance traffic) between any two given cities, we estimate these numbers using our algorithm given in the Supplemental material [40]. The basic idea behind the algorithm is that most people prefer road for distances of < 300 Kms. This algorithm gives us daily traffic of around 25 Lakhs per day. If we assume that ten toll booths are encountered on average while travelling by National highways, the daily short-distance traffic on National highways comes out to around 23 Lakhs, based on some assumptions about Passenger Car Unit [44]. According to some unofficial sources, National highways carry around 40% of the total road traffic [45]. This implies that 60% or about 34 Lakhs/day is carried by the state highways and other roads. Given that, we are ignoring many small towns/villages with a population of less than 1 Lakh, as well as road transports for long distance, 25 Lakh passengers per day is a reasonable estimate for daily road traffic [refer table (1)].

All these data are assembled together to obtain the averaged daily traffic matrix \mathbf{F} , whose element F_i^j represents the mean composite volume of traffic (number of people) in the route from city i to j in a “typical” day. Note that the data is mainly drawn from or estimated for pre-covid years, 2017 to 2019. Figure 1 shows a snapshot of the averaged composite transportation network data. This combines the air, train and road mobilities of people for the largest 500 connections (or edges) in terms of the volume

of people carried in that route. This can be thought of as the daily mean dominant mobility mode of the people in India. Based on this dataset, we find that $F_i^j \neq F_j^i$, *i.e.*, it is a directed network, implying that the number of people travelling from city i to j and vice-versa are not equal. Indeed, the lines drawn in Fig. 1 are also averaged over both directions. The line thickness indicates its weight - thicker lines represent more people travelling in that route. In this paper, we will also neglect the different time-scales associated with various modes of transport (e.g., the air is faster than train or road travel) and focus only on the average number of people travelling in a day.



Figure 1: An averaged composite transportation network of India with data largely drawn from or estimated for pre-covid years 2017 to 2019. The lines represent the connections between cities and their thickness indicates its relative importance – the thicker the line, the more people travel in that route. To avoid clutter, this figure shows only the top 500 of the 23224 undirected connections in the network. This plot along with the rest of the map plots in the paper are made using Leaflet [46].

4 Infectious diseases hazard index

The central idea in constructing the hazard map is the notion of *effective distance* first introduced in Ref. [12]. If F_i and F^i , respectively, denote the total number of people travelling out of and into city i , then the one-step conditional probability that a person leaving city i travels to city j is given by

$$P_i^j = \frac{F_i^j}{F_i}. \quad (6)$$

Note that P_i^j defined above is related to W_i^j used in Eq. (2) as,

$$W_i^j = \gamma_i P_i^j, \text{ where } \gamma_i = \frac{F_i}{N_i} \quad (7)$$

is also called the local mobility. In terms of P_i^j , the mobilities based “distance” d_i^j between cities i and j is

$$d_i^j = 1 - \log P_i^j. \quad (8)$$

If two cities a and b are not directly connected and hence no one directly travels from a to b , then $P_a^b = 0$, and yields the distance to be $d_i^j \rightarrow \infty$. In practice, even if two cities are not directly connected, the infection will still spread through alternative edges and nodes. All such connections are considered by defining $\{\Gamma_i^j\}$ as all possible paths between city i and j . This is denoted by $\lambda(\Gamma)$ and represents the sum of d_i^j 's for all the successive pairs of cities along a path. Thus, for a given pair of cities, there would be multiple distances depending on the path taken. The effective distance D_{eff} is defined as the minimum out of all possible distances :

$$D_i^j = \min_{\Gamma} \lambda(\Gamma). \quad (9)$$

Physically, this notion of effective distance incorporates the fact that the spread of infection is dependent on the flux of people rather than the geographical distance. This has the following implication – starting with the outbreak location, some of the geographically farther places can get the infection earlier than the neighbouring places due to their shorter effective distance from the outbreak location. *The time of arrival* T_A of the infection to a certain city is defined as the first time when the instantaneous number of (active) infected cases crosses a predefined threshold I_c , *i.e.*, $I(t) > I_c$, or the first passage time in the language of statistical physics. By this criteria, on a fully connected network, all the nodes will eventually get infected. The time of arrival of infection T_A at location b from an outbreak location a will depend on the effective distance D_a^b . Remarkably, for a wide range of realistic α and β , it is seen that $T_A \propto D_a^b$. Further, if the reproduction number $R_0 = \alpha/\beta > 1$, then all the cities eventually get infected provided the transportation network is fully connected. However, the time of arrival is usually non-trivial and does not reveal systematics with respect to parameters in the model. The ability to predict the arrival of infection at a given location in a spatially extended system is not only of academic interest but also has far-reaching real-life practical consequences.

As we demonstrate below in Fig. 2, the effective distance D_{eff} is strongly correlated with time of arrival T_A (since the time of outbreak), and hence in principle we can use either D_{eff} or T_A as an indicator of the hazard of a city with respect to a given outbreak location. While D_{eff} is based on mobility patterns, T_A depends on infection parameters α and β . In this work, by construction, $D_{\text{eff}} = 0$ for the outbreak location itself and carries the biggest hazard value. Large values of D_{eff} imply lesser hazard. In the extreme case, if $D_{\text{eff}} = \infty$, then this location will never get infected. This will typically happen only for isolated towns/cities with no connectivity to the rest of the world. In contrast, smaller values of D_{eff} imply that infection will reach more quickly, and they face relatively more hazard. For visual depiction, it is convenient to use a hazard index defined as $h = \exp(-D_{\text{eff}})$. Thus, the disease outbreak location has the maximum hazard index $h = 1$, while an unconnected town with $D_{\text{eff}} = \infty$ will have a minimum value of $h = 0$. A city has a greater hazard if the hazard value h assigned to it is closer to 1.

In this paper, since the quantity of interest is the hazard index for every city obtained from averaged transportation data, we will neglect the different time scales associated with various modes of transport. Thus, for instance, travel time differences via airline and railway mode are ignored because the mobility data we use is averaged over longer timescales than these travel times. The coupled differential equations given by Eq. (4) are numerically solved using the fourth-order Runge-Kutta method. The initial conditions are assumed to be consistent with the choice of any one city as an outbreak location. At the city of disease outbreak, the number of infected persons is taken to be $I(t = 0) = I_0$, and at all the other cities $I(0) = 0$. The choice of outbreak location is a parameter in the problem. For this choice of outbreak location and other model parameters α and β , the solution time-series $I(t)$ is computed for all cities for $t > 0$. Fixing the threshold I_c for instantaneous active cases, time of arrival T_A is computed. As will be shown below, the time of arrival strongly correlates with effective distance D_{eff} but not with the geographical distance D_{geo} .

5 Results

For the results shown in the rest of the paper, the time of arrival is defined to be the time when the infection exceeds the threshold $I_c = 10$ for the first time. The SIR model parameters are fixed at $\alpha = 1.5, \beta = 1.0$, which gives $R_0 = 1.5$, a typical value that was witnessed for SARS-CoV-2 during the first wave in many countries, including India. In Fig. (2) (left panel), the effective distance $D_{i_0}^j$, where i_0 is the declared outbreak location of the infectious disease, is plotted as function of the time of arrival T_A^j at city j . This is shown for four different choices of outbreak locations (two metros, a smaller city, and a big town), namely, (a) Delhi, (b) Mumbai, (c) Patna and (d) Tirupati. The initial infected fraction at the outbreak location is set at 0.0001, *i.e.*, at $t = 0$, $I_{i_0}/N_{i_0} = 0.0001$. This reveals a good linear relation between $D_{i_0}^j$ and T_A^j , and the regression coefficients of at least 0.94 in each case, provides a quantitative confirmation. For comparison, on the right panel of this figure, geographical distance from the city j is shown as a function of time of arrival T_A^j . The clutter of points and the regression coefficient ≈ 0.0 both point to no relationship between the time of arrival of infectious disease and geographical distance from the city/town of disease outbreak. Thus, the geographical distance is not a good measure for predicting the spread of the infection, a result known for the case of infection spread through air travel alone [12]. Remarkably, even in a heterogeneous country like India, where air travel is by far the least popular mode of transport, accounting for less than 1% of all mobility, the linearity holds good.

In Table 2, the time of arrival is shown for the same set of outbreak locations shown in Fig. 2. The list of the top ten cities/towns that face the hazard with respect to a given outbreak location is also listed. Clearly, for outbreaks taking place in small towns, the surrounding regions face the first brunt of infection, and the infection takes some time to reach the bigger cities. On the other hand, if big metros are the outbreak locations, they quickly reach far corners of the country. For instance, infection starting at Tirupati reaches Bangalore in about Five days, whereas if Mumbai or Delhi is the epicentre,

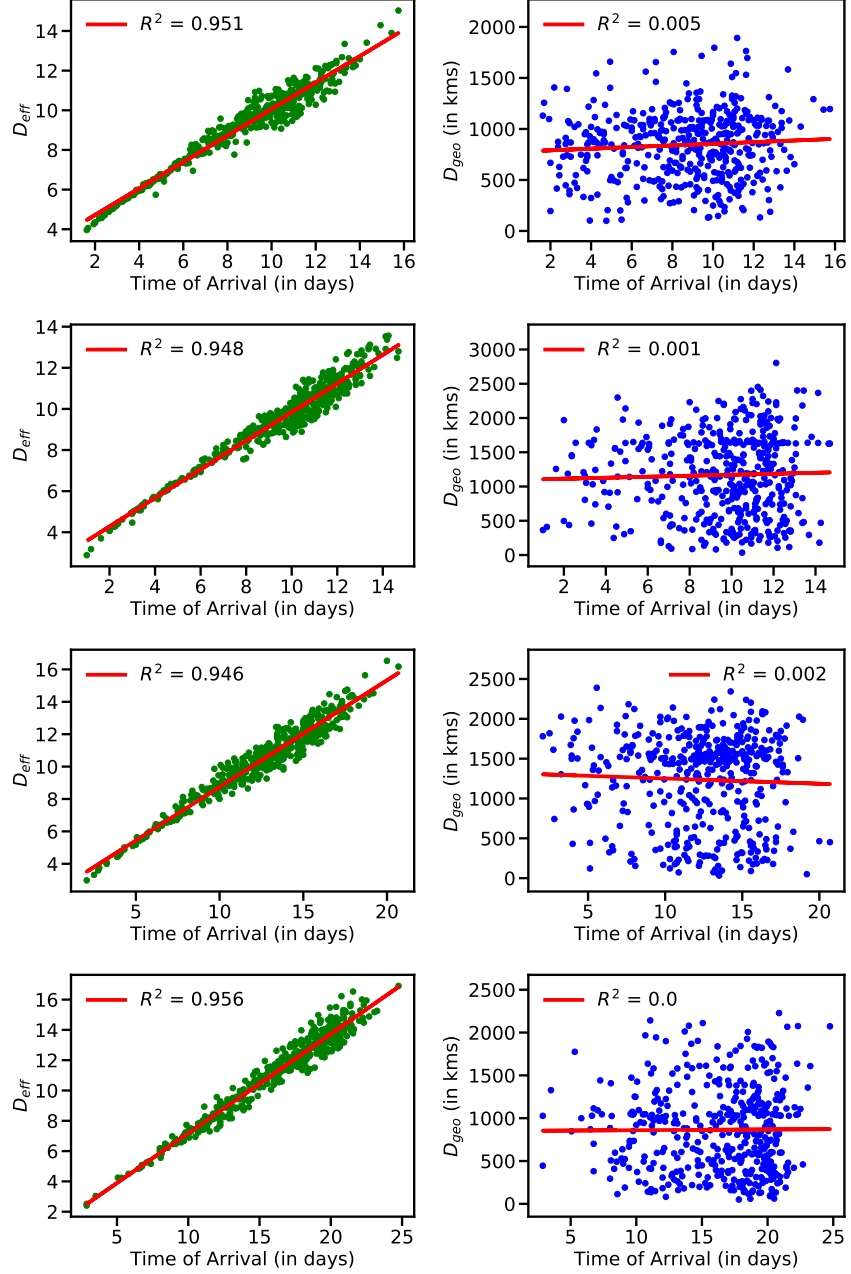


Figure 2: The effective distance $D_{i_0}^j$ compared to the geographical distance from the outbreak location. Left column (green circle) shows the effective distance $D_{i_0}^j$ as a function of time of arrival of the infection at city j from outbreak location city i_0 . We get time of arrival by numerically solving Eq. (4). The parameters are $\alpha = 1.5, \beta = 1.0, I_c = 10$. Outbreak locations from top to bottom are Delhi, Mumbai, Patna and Tirupati. The right column shows the geographical distance D_{geo} from i_0 plotted against time of arrival. Red line is obtained through a linear regression, with regression coefficient given by R^2 .

it spreads to Bangalore in about 2.5 days. The hazard map in Fig. 3 shows this information and data in an appealing visual form for the same four outbreak locations (shown using black location icon). The size of circles drawn in this figure is indicative of the hazard index – the larger the circle, the greater is the hazard. For a given outbreak location, the hazard index for all the rest of the cities/towns was calculated, but only the top 10 cities/towns are shown in this figure to avoid clutter.

To get further insight into how the infectious diseases hazard map representation works, it is instructive to visualise the hazard map assuming only the air, railway or road transport is operating. Using the framework proposed in this work, this can be easily done by constructing the traffic matrix \mathbf{F} using mobility data from only one of the transportation modes, namely, air, train or road. By going through the rest of the procedure given in section 4, the transportation-mode specific hazard map is depicted for two different outbreak location, for Bangalore in Fig. 4, and for Guwahati in Fig. 5. For comparison, the composite hazard constructed using all the transport modes is also shown in these figures. It is obvious that air transport has the largest reach. If only the mobility by air is considered with Bangalore as an outbreak city, then even the farthest cities like Delhi, Kolkata and Mumbai display high hazard values. In comparison, if train mobility alone is considered, most of the high hazard cities in the top-10 list are located within south India. It must be noted that cities like Mumbai and Delhi would still have significant hazard values, but they do not figure in the top-10 list. A similar scenario is seen in the case of the road mobility hazard map. Since the volume of people carried by train and road is much larger than air, the hazard values indicated in the composite hazard map shows that train and road transport together are major carriers of infection than the air transport. The results for a similar exercise performed with Guwahati as the outbreak location is shown in Fig. 5. The same conclusion can be inferred from this figure as well. This scenario repeats for all the outbreak locations. Some of the earlier works that used mobility to discuss infectious diseases spread have primarily and often exclusively used only airline mobility, and to an extent, it might be justified in the context of Europe and America [12]. India has not just one of the largest railway networks but also one used by a significant fraction of people. Hence, an analysis of this type presented in this paper is most desirable in the Indian context.

Finally, in Table (3), the results of our framework are compared with real data of T_A for the first wave of the SARS-CoV-2 pandemic in India in 2020. The data for active infected cases is obtained from a private API-based website [2]. However, this is district-level data and is available from 26th April-2020. In order to work with the available data, it is assumed that there is only one city per district with a population higher than 1 Lakh. Mumbai was seen to cross the threshold first, and hence, Mumbai is taken to be the outbreak location. There were ~ 4000 active infected cases in Mumbai on 26th April 2020, which was taken as an initial condition at $t = 0$ for this real-life data. The Time of Arrival is computed from the number of infected cases averaged over three days, and the threshold is fixed at $I_c = 4000$. Thus, we obtained T_A for 236 out of 446 cities using the observed data. A similar scenario was replicated in the simulation framework. Mumbai is taken as the outbreak location and other parameters are taken to be $\alpha = 1.15, \beta = 1.0, I_c = 4500$. These parameters were chosen so that T_A is of a similar order of magnitude

| Delhi | |
|-----------|------|
| City | TOA |
| Kanpur | 1.62 |
| Mumbai | 1.69 |
| Gurgaon | 1.94 |
| Faridabad | 2.00 |
| Lucknow | 2.00 |
| Jhansi | 2.19 |
| Rohtak | 2.31 |
| Ludhiana | 2.38 |
| Bangalore | 2.38 |
| Moradabad | 2.44 |
| Meerut | 2.44 |
| Kolkata | 2.62 |

| Mumbai | |
|------------------|------|
| City | TOA |
| Thane | 1.00 |
| Pune | 1.19 |
| Delhi | 1.62 |
| Ahmedabad | 2.00 |
| Surat | 2.00 |
| Pimpri Chinchwad | 2.19 |
| Nashik | 2.25 |
| Bangalore | 2.38 |
| Vasai | 2.38 |
| Hyderabad | 2.56 |
| Chennai | 2.94 |
| Vasco Da Gama | 3.00 |

| Patna | |
|-----------------|------|
| City | TOA |
| Gaya | 2.06 |
| Dinapur Nizamat | 2.50 |
| Arrah | 2.75 |
| Delhi | 2.81 |
| Bhagalpur | 3.25 |
| Kolkata | 3.25 |
| Darbhanga | 3.88 |
| Biharsharif | 3.94 |
| Jehanabad | 3.94 |
| Begusarai | 4.00 |
| Muzaffarpur | 4.06 |
| Varanasi | 4.06 |

| Tirupati | |
|----------------|------|
| City | TOA |
| Chittoor | 2.88 |
| Chennai | 2.88 |
| Hyderabad | 3.50 |
| Bangalore | 5.06 |
| Vellore | 5.31 |
| Tiruvannamalai | 5.81 |
| Kadapa | 6.50 |
| Vijayawada | 6.62 |
| Visakhapatnam | 6.75 |
| Anantapur | 6.75 |
| Madanapalle | 6.75 |
| Nellore | 7.06 |

Table 2: Time of Arrival (T_A), in days, for each of the four outbreak locations in Fig. 2, shown only for cities that have largest 10 values of T_A . The parameters are $\alpha = 1.5$, $\beta = 1.0$, and $I_c = 10$.

as the real data. From this simulation, the time of arrival is computed for all the cities on the network. Both the results are compared in Table (3). We compare the top 12 cities in both the list to see how well they match. We note that only Surat, Pimpri-Chinchwad, and Vasai feature in simulation outcome but not in the observed data. However, Pimpri-Chinchwad and Pune are considered separate cities in

simulation but represent the same Pune district real data. Thus, in a way, even Pimpri-Chinchwad appears to be hidden in real data. Hence, 9 out of 11 (without counting Mumbai) cities are common in both the hazard lists. This puts the similarity of the two lists at around 81%. Yet, the hazard ranking of cities does not quite match up very well. Though the comparison is coarse, it is remarkable that 80% of cities obtained from simulations match with those in the list obtained from real data. Given the levels of approximations made in the simulation framework and the uncertainties in the data, it provides the first proof-of-concept that it is possible to create a systematic framework for predicting the hazard arising from the spread of infectious diseases in India [47]. If reliable transportation and epidemiological data become available, it might be possible to obtain reliable hazard prediction.

| City | Simulation TOA | City | Real TOA |
|------------------|----------------|-----------|----------|
| Mumbai | 1 | Mumbai | 1 |
| Pune | 22 | Delhi | 11 |
| Thane | 23 | Ahmedabad | 13 |
| Delhi | 25 | Chennai | 16 |
| Ahmedabad | 26 | Thane | 25 |
| Surat | 26 | Pune | 46 |
| Bangalore | 27 | Hyderabad | 57 |
| Pimpri Chinchwad | 28 | Bangalore | 65 |
| Hyderabad | 29 | Guwahati | 70 |
| Nashik | 29 | Kolkata | 79 |
| Vasai | 30 | Nashik | 85 |
| Chennai | 31 | Guntur | 88 |

Table 3: Comparison of the time of arrival of infection for real data and that from the simulation framework proposed in this work. The *Time of Arrival* is given in days. Note that 9 out of 11 cities are common to both the lists, showing that the proposed framework has predictive capability.

6 Conclusion

If an infectious disease breaks out in one city, how long does it take to for the infection to reach other cities and towns? This length of time can be a measure of the hazard that can be assigned to other cities – the longer it takes, the lesser the hazard. Based on this idea, an infectious disease hazard map for India using the data from the transportation network has been proposed and implemented. The key idea is the notion of effective distance D_{eff} , as opposed to geographical distance, between the outbreak city and other cities. This measure D_{eff} depends on the averaged transportation and mobility pattern of people. The real data from air, road, and rail transportation networks are incorporated to estimate the hazard index for 446 cities/towns in India with a population of 1 Lakh or more. We have relied on the available,

and in some cases scanty, data sources and constructed transport algorithms to aggregate mobility data between any two cities. Using the SIR compartmental model coupled with this movement dynamics across the cities, it is shown that infection spread correlates much better with effective distance D_{eff} rather than geographical distance. The hazard value is determined by considering D_{eff} as a proxy for the time taken for the infection to arrive at other cities/towns. The hazard map for a few outbreak locations are shown and is also compared with the real-life data for the first wave of SARS-CoV-2 in India. The coarse agreement between the two shows that this approach is capable of predicting hazards due to infectious diseases. This framework can be extended to include multiple disease outbreak locations, and identify effective ways to selectively block transport to arrest the quick spread of the disease. Some of these will be addressed in subsequent publications.

Acknowledgments

This work was funded by a special MATRICS grant MSC/2020/000122 given by SERB, Government of India to MSS, GJS and SJ. OS would like to thank Aanjaneya Kumar and Suman Kulkarni for the discussions. OS and MB acknowledge the INSPIRE grant from the Department of Science and Technology, India.

References

- [1] <https://covid19.who.int/>, <https://coronavirus.jhu.edu/map.html>
- [2] <https://www.covid19india.org/>
- [3] Belik, V., Geisel, T., Brockmann, D., Natural human mobility patterns and spatial spread of infectious diseases. *Physical Review X* **1**, 011001. (2011)
- [4] Coltart, C.E., Behrens, R.H., The new health threats of exotic and global travel. *British Journal of General Practice* **62**, 512–513. (2012)
- [5] Helbing, D., Globally networked risks and how to respond. *Nature* **497**, 51–59. (2013)
- [6] Barbosa, H., Barthelemy, M., Ghoshal, G., James, C.R., Lenormand, M., Louail, T., Menezes, R., Ramasco, J.J., Simini, F., Tomasini, M., 2018. Human mobility: Models and applications. *Physics Reports* **734**, 1–74. (2018)
- [7] I. D. Mills, The 1918-1919 influenza pandemic - The Indian experience, *The Indian Economic and Social History Review* **23**, 1 (1986). <https://doi.org/10.1177%2F001946468602300102>
- [8] The Annual Report of the Sanitary Commissioner with the Government of India (1918), (Calcutta, 1920).

- [9] Gautreau, A., Barrat, A., Barthelemy, M., Global disease spread: statistics and estimation of arrival times. *Journal of theoretical biology* **251**, 509–522. (2008)
- [10] Barthélemy, M., Spatial networks. *Physics Reports* **499**, 1–101. (2011)
- [11] Feng, L., Zhao, Q., Zhou, C., Epidemic in networked population with recurrent mobility pattern. *Chaos, Solitons & Fractals* **139**, 110016. (2020)
- [12] Brockmann, D., Helbing, D., The Hidden Geometry of Complex, Network-Driven Contagion Phenomena. *Science* **342**, 1337–1342. (2013)
- [13] Arenas, A., Cota, W., Gómez-Gardeñes, J., Gómez, S., Granell, C., Matamalas, J.T., Soriano-Paños, D., Steinegger, B., Modeling the Spatiotemporal Epidemic Spreading of COVID-19 and the Impact of Mobility and Social Distancing Interventions. *Physical Review X* **10**, 041055. (2020)
- [14] Althouse, B.M., Wenger, E.A., Miller, J.C., Scarpino, S.V., Allard, A., Hébert-Dufresne, L., Hu, H., Stochasticity and heterogeneity in the transmission dynamics of SARS-CoV-2. [arXiv:2005.13689](https://arxiv.org/abs/2005.13689). (2020)
- [15] Garcia-Gasulla, D., Napagao, S.A., Li, I., Maruyama, H., Kanezashi, H., P'erez-Arnal, R., Miyoshi, K., Ishii, E., Suzuki, K., Shiba, S., Global Data Science Project for COVID-19 Summary Report. [arXiv:2006.05573](https://arxiv.org/abs/2006.05573). (2020)
- [16] R. Gopal, V. K. Chandrasekar and M. Lakshmanan, Dynamical modelling and analysis of COVID-19 in India, *Current Science* **120** 1342 (2021).
- [17] Bedi, P., Gole, P., Gupta, N., Jindal, V., Projections for COVID-19 spread in India and its worst affected five states using the Modified SEIRD and LSTM models. [arXiv:2009.06457](https://arxiv.org/abs/2009.06457). (2020)
- [18] Khajanchi, S., Sarkar, K., Forecasting the daily and cumulative number of cases for the COVID-19 pandemic in India. *Chaos: An Interdisciplinary Journal of Nonlinear Science* **30**, 071101. (2020)
- [19] Das, A., Dhar, A., Goyal, S., Kundu, A., Pandey, S., COVID-19: Analytic results for a modified SEIR model and comparison of different intervention strategies. *Chaos, Solitons & Fractals* **110595**. (2021)
- [20] Jha, V., Forecasting the transmission of Covid-19 in India using a data driven SEIRD model. [arXiv:2006.04464](https://arxiv.org/abs/2006.04464). (2020)
- [21] Khajanchi, S., Sarkar, K., Mondal, J., Perc, M., Dynamics of the COVID-19 pandemic in India. [arXiv:2005.06286](https://arxiv.org/abs/2005.06286). (2020)
- [22] Mishra, R., Gupta, H.P., Dutta, T., Analysis, Modeling, and Representation of COVID-19 Spread: A Case Study on India. [arXiv:2008.13116](https://arxiv.org/abs/2008.13116). (2020)

- [23] Sarkar, K., Khajanchi, S., Nieto, J.J., Modeling and forecasting the COVID-19 pandemic in India. *Chaos, Solitons & Fractals* **139**, 110049. (2020)
- [24] Pujari, B.S., Shekatkar, S., Multi-city modeling of epidemics using spatial networks: Application to 2019-nCov (COVID-19) coronavirus in India. medRxiv. <https://doi.org/10.1101/2020.03.13.20035386> (2020)
- [25] Gupta, S., Shah, S., Chaturvedi, S., Thakkar, P., Solanki, P., Dibyachintan, S., Roy, S., Sushma, M.B., Godbole, A., Jaseem, N. *et. al.*, An India-specific compartmental model for Covid-19: projections and intervention strategies by incorporating geographical, Infrastructural and response heterogeneity. [arXiv:2007.14392](https://arxiv.org/abs/2007.14392). (2020)
- [26] Earthquake hazard maps by the United States Geological Survey <https://www.usgs.gov/natural-hazards/earthquake-hazards/maps>
- [27] <https://censusindia.gov.in/2011-common/censusdata2011.html>
- [28] Gong, Y., Song, Y., Jiang, G., Epidemic spreading in metapopulation networks with heterogeneous infection rates, *Physica A: Statistical Mechanics and its Applications*, **416**, 208-218. (2014)
- [29] Ronald, R., and Hilda, P., An application of the theory of probabilities to the study of a priori pathometry.–Part III *Proc. R. Soc. Lond. A* **93**: 225–240. (1917)
- [30] Kermack, W. O. and McKendrick, A. G., A contribution to the mathematical theory of epidemics, *Proc. R. Soc. Lond. A* **115**:700–721. (1927)
- [31] Colizza, V., Pastor-Satorras, R., and Vespignani, A. Reaction-diffusion processes and metapopulation models in heterogeneous networks. *Nature Phys* **3**, 276–282 (2007).
- [32] Taylor, D., Klimm, F., Harrington, H.A., Kramár, M., Mischaikow, K., Porter, M.A., Mucha, P.J., 2015. Topological data analysis of contagion maps for examining spreading processes on networks. *Nature communications* **6**, 1–11. (2015)
- [33] Tolić, D., Kleineberg, K.-K., Antulov-Fantulin, N., Simulating SIR processes on networks using weighted shortest paths. *Scientific reports* **8**, 1–10. (2018)
- [34] https://indianrailways.info/all_trains/
- [35] <https://www.makemytrip.com/railways/list-of-indian-railway-stations.html>
- [36] <https://enquiry.indianrail.gov.in/mntes/>
- [37] Rajput, N.K., Badola, P., Arora, H., Grover, B.A., Complex Network Analysis of Indian Railway Zones. [arXiv:2004.04146](https://arxiv.org/abs/2004.04146). (2020)

- [38] Gopalakrishnan, R., Rangaraj, N., Capacity management on long-distance passenger trains of Indian Railways. *Interfaces* **40**, 291–302. (2010)
- [39] Sen, P., Dasgupta, S., Chatterjee, A., Sreeram, P.A., Mukherjee, G., Manna, S.S., Small-world properties of the Indian railway network. *Physical Review E* **67**, 036106. (2003)
- [40] Please refer to the Supplementary material.
- [41] https://indianrailways.gov.in/railwayboard/uploads/directorate/stat_econ/IRSP_2016-17/Facts_Figure/Fact_Figures%20English%202016-17.pdf, Page no. 6.
- [42] <http://www.knowindia.net/aviation.html>
- [43] https://www.civilaviation.gov.in/sites/default/files/MoCA_Annual_Report_2018_19.pdf, Page No. 49
- [44] <https://tis.nhai.gov.in/>
- [45] https://en.wikipedia.org/wiki/Transport_in_India
- [46] Leaflet — Map tiles by Stamen Design, under CC BY 3.0. Data by © OpenStreetMap, under CC BY SA.
- [47] For more information, visit <https://www.iiserpune.ac.in/~hazardmap/>

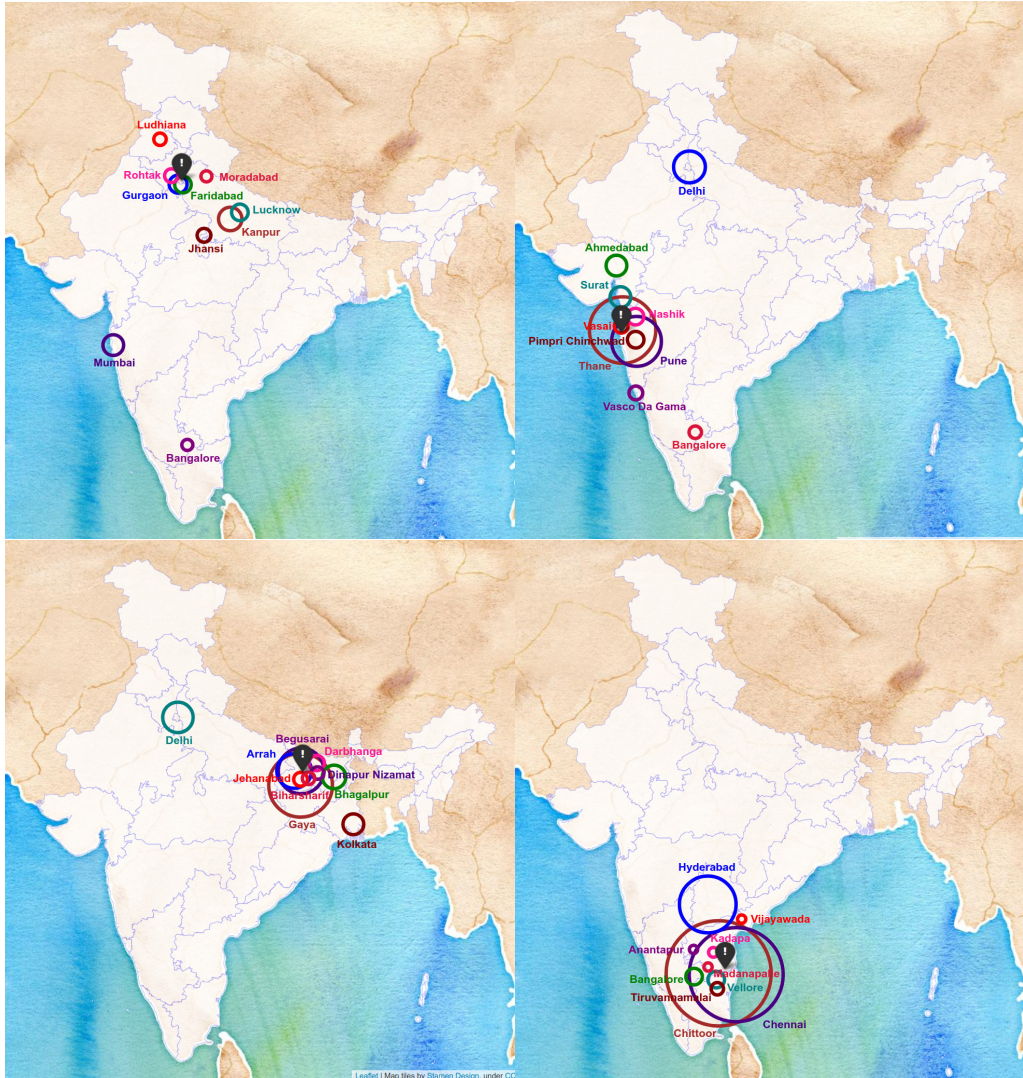


Figure 3: A visual depiction of the information in Table (2) in the form of an infectious diseases hazard map, with outbreak locations at Delhi, Mumbai, Patna and Tirupati (shown as black coloured location icon). The radius of circle is proportional to the hazard index of the city/town. Larger the circle, greater is the hazard and their colour does not carry any information. Only the cities/towns with top-10 hazard values are shown.

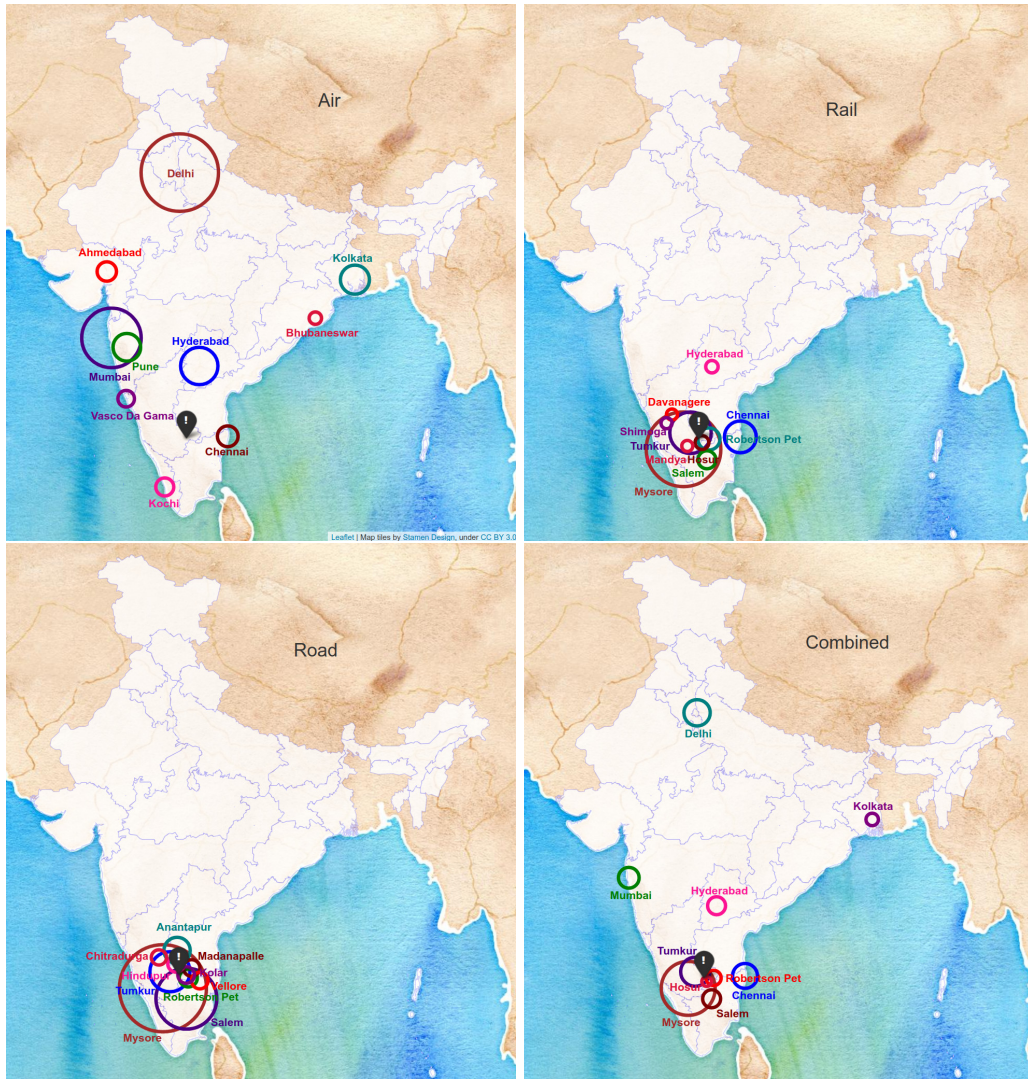


Figure 4: Transportation mode specific Hazard maps with Bangalore as outbreak location. The figures correspond to Air, Rail transport in the top panel, and Road and Combined modes of transport in the bottom panel. The radius of circle is proportional to the hazard index of the city/town. Larger the circle, greater is the hazard and their colour does not carry any information. Only the cities/towns with top-10 hazard values are shown.

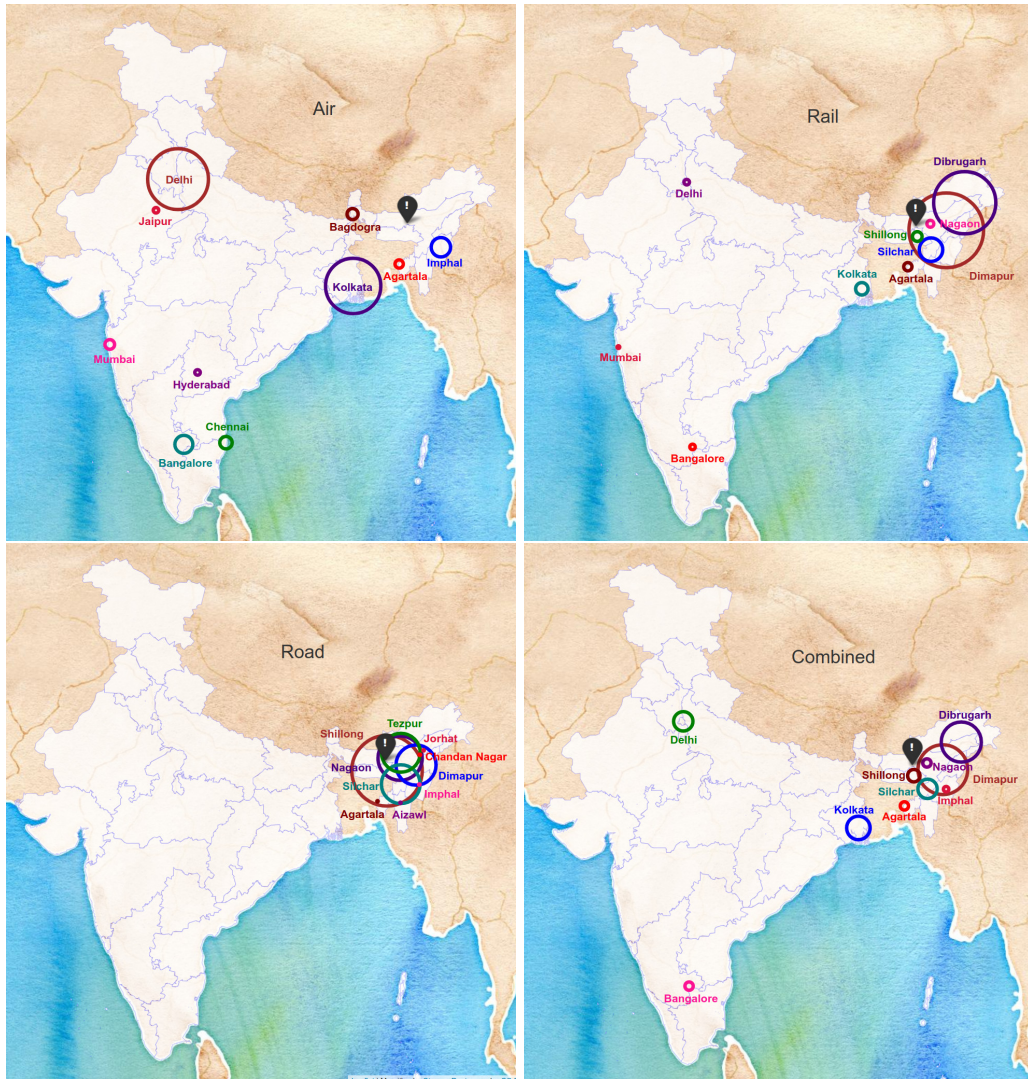


Figure 5: Transportation mode specific Hazard maps with Guwahati as outbreak location. The figures correspond to Air, Rail transport in the top panel, and Road and Combined modes of transport in the bottom panel. The radius of circle is proportional to the hazard index of the city/town. Larger the circle, greater is the hazard and their colour does not carry any information. Only the cities/towns with top-10 hazard values are shown.

SUPPLEMENTAL MATERIAL FOR
**An infectious diseases hazard map for India based on mobility and
transportation networks**

1 Algorithms

The raw data that we have collected is not in the format of number of passengers travelling from city i to city j except for the airway. The rail data is in the form of travel routes, while there is no reliable source for road data. In this supplemental material, we will look at two algorithms to estimate the road and rail traffic matrices entries by making some reasonable assumptions.

1.1 Railways

The raw data for railways is in the format of the train routes with stops [1, 2]. We have the population for each of the stop on all routes. The raw data set consists of 4480 routes, including both forward and backward routes [3]. To make the data-analysis tractable, we include only those cities that have a population of more than 1 Lakh as per the 2011 census in India [4]. Thus, few smaller sub-stations in the vicinity of major metropolitan cities are also treated as separate cities.

To extract data from train routes and population of cities, we rely on the two assumptions,

1. The train is always full while travelling between any two consecutive cities.
2. The number of people travelling between any two cities (not necessarily consecutive) on a route is proportional to their individual populations.

In addition to the information about the route and population, we also have the information about the weekly frequency and the type of train on each of the routes. We use the knowledge about the train type to fix the capacity of each train. We will now delve into the details of the algorithm.

Let us consider a particular route with k stations labelled by indices 1, 2, ..., k . The population of the cities is N_1, N_2, \dots, N_k respectively. Assumption 1 tells us that the train starts with full capacity from city 1, which we denote by C . According to the assumption 2 these C number of people will get down at remaining stations proportional to the population. Going back to our first assumption; the number of people getting on the train at any city j ($j \geq 2$) would be the same as number of people getting down at that station. Let \mathbf{F} denote the traffic matrix, where F_i^j corresponds to number of people going from city i to city j in unit time. Similarly, F_i represents the total number of people moving out of city i in a unit amount of time.

Now, the number of people getting on the train at city 2, will again get down at cities j ($j \geq 3$), proportional to their population. The number of people getting down at city 3 would be dependent on number of people who got on the train in city 1 and 2. Thus, we continue this process until city $k - 1$, and finally C number of people will get down at city k . The total outgoing/incoming number of people for the cities on the route can be expressed mathematically as,

$$\begin{aligned}
 F_1 &= C, \\
 F_2 &= F_1 \frac{N_2}{\sum_{j=2}^k N_j}, \\
 F_3 &= F_1 \frac{N_3}{\sum_{j=2}^k N_j} + F_2 \frac{N_3}{\sum_{j=3}^k N_j}, \\
 F_4 &= F_1 \frac{N_4}{\sum_{j=2}^k N_j} + F_2 \frac{N_4}{\sum_{j=3}^k N_j} + F_3 \frac{N_4}{\sum_{j=4}^k N_j}, \\
 &\vdots
 \end{aligned}$$

$$F_a = \sum_{i=1}^{a-1} \left[F_i \frac{N_a}{\sum_{j=i+1}^k N_j} \right]. \quad (1)$$

We note that these equations have a recursive form. Luckily, we can simplify each of them to get a simple form for F_a , which denotes the total number of people leaving city a ,

$$\begin{aligned} F_a &= F_1 \frac{N_a}{\sum_{j=a}^k N_j} = C \frac{N_a}{\sum_{j=a}^k N_j}, & \text{for, } 2 \leq a \leq k-1, \\ F_a &= F_1 = C, & \text{for, } a = 1. \end{aligned} \quad (2)$$

For instance the expression for F_3 can be simplified as,

$$\begin{aligned} F_3 &= F_1 \frac{N_3}{\sum_{j=2}^k N_j} + F_2 \frac{N_3}{\sum_{j=3}^k N_j}, \\ F_3 &= F_1 \frac{N_3}{\sum_{j=2}^k N_j} + F_1 \frac{N_2}{\sum_{j=2}^k N_j} \frac{N_3}{\sum_{j=3}^k N_j}, \\ F_3 &= F_1 \frac{N_3}{\sum_{j=2}^k N_j} \left[1 + \frac{N_2}{\sum_{j=3}^k N_j} \right], \\ F_3 &= F_1 \frac{N_3}{\sum_{j=2}^k N_j} \left[\frac{\sum_{j=2}^k N_j}{\sum_{j=3}^k N_j} \right], \\ F_3 &= F_1 \frac{N_3}{\sum_{j=3}^k N_j}. \end{aligned} \quad (3)$$

The number of people going from city a to city b ($2 \leq a < b \leq k$) for this route would be,

$$\begin{aligned} F_a^b &= \left[C \frac{N_a}{\sum_{j=a}^k N_j} \right] \left[\frac{N_b}{\sum_{j=b+1}^k N_j} \right], & \text{for, } 2 \leq a < b \leq k, \\ F_a^b &= \left[C \frac{N_b}{\sum_{j=a+1}^k N_j} \right], & \text{for, } 1 = a < b \leq k. \end{aligned} \quad (4)$$

Thus, we have obtained the expression for number of people travelling from city a to city b for a given route. There is only one free parameter in the above expression $F_1 = C$, which we fix by knowing the type of train and its capacity [1]. We can run the same algorithm for all the routes in our raw data-set to get the full \mathbf{F} -matrix for railway as the mode of transport. We illustrate this algorithm in a more visual and simple way, using an imaginary toy route and population in Fig. (1).

Let us consider a train route going through 4 cities A, B, C, and D having equal population N . We will also assume that the capacity of train is 120. Figure. (1) shows the final results after running the algorithm for the forward and backward routes. As we can readily see the \mathbf{F} -matrix is not symmetric even if we consider the simplest case of just one route through cities of equal population. It is also worth noting that the total number of people travelling in/out of a city is not proportional to the city population. The assymetricity of \mathbf{F} -matrix and unequal local mobility becomes more pronounced when we consider all cities and all the routes.

1.2 Road

In this section, we will look at the algorithm used to generate the road traffic. To our knowledge, there is no systematic source of road traffic connecting almost all cities in India with population above 1 Lakh. The only available data is about toll booths on national highways [5]. This data is not useful as it leaves out most of the short-distance routes. Thus, we have to estimate the traffic data by using the available information.

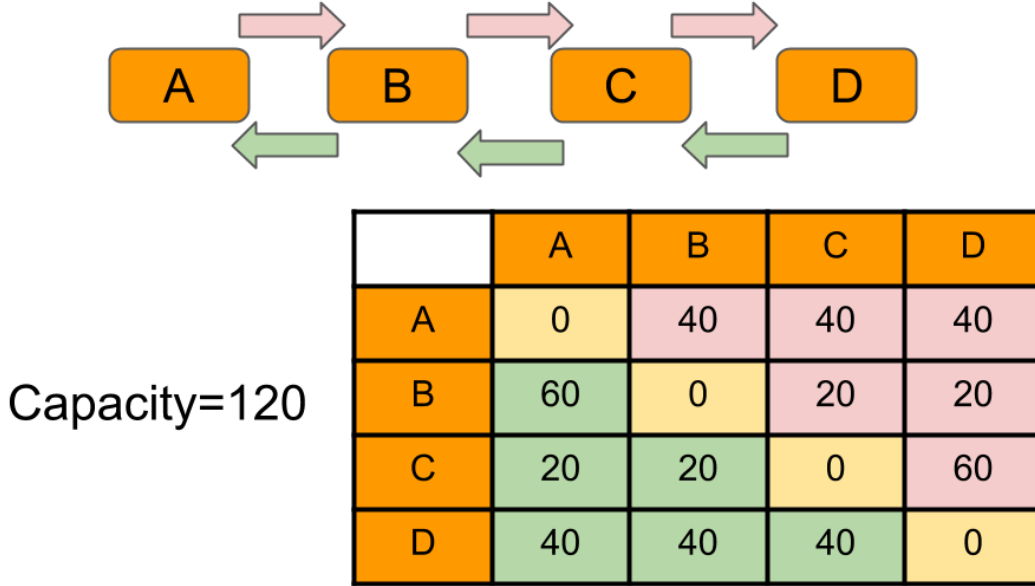


Figure 1: Model Train Algorithm: We consider two routes here: A-B-C-D and D-C-B-A. For simplicity let us assume that the population of all four cities is equal and the capacity of the train is 120. We run the algorithm using Eq. (4) and each entry in the table T_{ij} specifies the number of people travelling from i to j . The colour in the table correspond to the route in the upper part of the figure.

As a simplest case, we assume that the final \mathbf{F} -matrix is symmetric. We can move away from this assumption, however, the process to make sure that the population of each city remains constant becomes more complex.

The next assumption we make is that most people use road travel for a short distance and long-distance travel is usually undertaken through railways or by aeroplane. And we make the final assumption that the total number of people travelling by road is proportional to the population of the city. We will later see how these specific assumptions help us fix the free parameters in our algorithms under the given set of constraints.

First we construct a graph of the cities. We consider cities within a specified distance as adjacent in this graph and construct an adjacency matrix for this graph. The distances are calculated using the latitudes and longitudes of the cities through the *geopy* library in python. Thus, the distances are not the lengths of the road between two cities, which in general would be more than the air distance. We then run an algorithm similar to the one we used for the train for this adjacency matrix.

Once we have the adjacency matrix, we sort the rows and columns according to the population. We start with the city with lowest population. We get the number of people travelling from this city by fixing a value for desired mobility and then distribute them to the cities adjacent to it proportional to their respective populations. We then make a symmetric entry in the \mathbf{F} -matrix. Next we move on to the city with second lowest population. We get the number of people travelling by multiplying the city population with the desired mobility. We subtract those people who are already accounted for through the symmetric entry in the first step, and distribute the rest proportionally same as before. We repeat this process, until we reach the most populous city. In case, the number of people accounted due to symmetric entry is higher than the desired mobility, we simply increase the mobility for that particular city by a small amount.

In order to understand this algorithm more clearly, we again give a toy example to illustrate our case in Fig. (3). We consider a network of 5 cities, such that the links AD, DA, BC, and CB are missing. The population of the five cities are in proportion as follows: A : B : C : D : E :: 10 : 25 : 50 : 75 : 100. Let's suppose that the population of city A is 1 Lakh and desired mobility is 0.0175. The algorithm proceeds as follows:

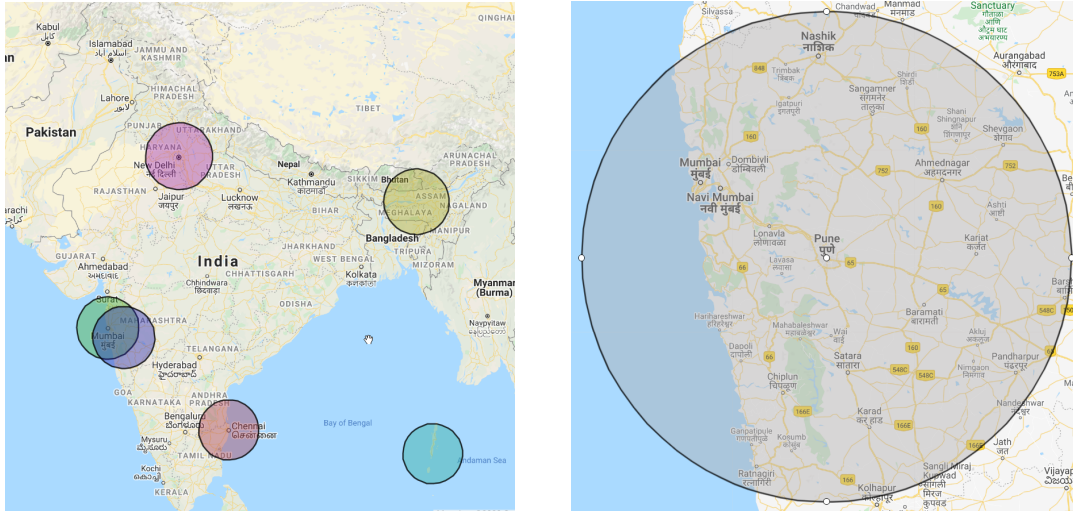


Figure 2: The relative size of 200 Kms circle for scale on map of India. On left hand side, we draw the circles around Mumbai, Pune, Delhi, Secennai, Guwahati, and Port-Blair. The right hand figure shows the circle for Pune. We can identify few of the important cities in Maharashtra which are connected to Pune by road from our algorithm.

- First we get the adjacency matrix whose indices are sorted according to the population. We start with lowest population city, i.e. A and distribute the desired number of people into all possible connections (blue coloured).
- We make symmetric entries in the first column (blue), subtract that number from desired traffic for city B and distribute the rest into possible connections (red). We make similar symmetric entry in red.
- For city C, we proceed as before, subtract, distribute, and make symmetric entry (yellow).
- We continue the algorithm until the table is fully filled.

| | A | B | C | D | E | Final | Desired |
|---|------|------|------|------|------|-------|---------|
| A | 0 | 250 | 500 | 0 | 1000 | 1750 | 1750 |
| B | 250 | 0 | 0 | 1768 | 2357 | 4375 | 4375 |
| C | 500 | 0 | 0 | 3536 | 4714 | 8750 | 8750 |
| D | 0 | 1768 | 3536 | 0 | 7821 | 13125 | 13125 |
| E | 1000 | 2357 | 4714 | 7821 | 0 | 15892 | 17500 |

Figure 3: Road Algorithm: The **F**-matrix for the toy model is symmetric and the final traffic, matches exactly with desired traffic for most cities.

Coming back to our algorithm for a network of 446 cities, the parameter values that we used in our algorithm are,

- desired mobility $\gamma = 0.015$.
- radius of circle of proximity = 200 Kms.
- The increase in traffic to distribute in case the symmetric entries already sum up more than the desired traffic was ($0.5 \times$ desired traffic).

According to [6], the total yearly road traffic in India is around 822 crore passengers. If we consider the average daily road traffic it comes out to be around 2.25 crore passengers. At a gross level, if we calculate the global mobility for India considering that the current population of 130 crores, we get the global mobility to be around 0.017. We take it to be 0.015 in order to compensate for fluctuations and other uncertainties.

We now mention few of the main results of the \mathbf{F} -matrix for road transport.

1. We increased the mobility of only 6 (out of 446) cities to account for overflow of traffic due to symmetric entries.
2. The cities have 20 connections on an average.
3. 92% (or ≈ 410) cities have a local mobility of 0.015. The average (global) mobility is 0.0115 and the standard deviation of it is 0.0021.

References

- [1] https://indianrailways.info/all_trains/
- [2] <https://www.makemytrip.com/railways/list-of-indian-railway-stations.html>
- [3] <https://enquiry.indianrail.gov.in/mntes/>
- [4] <https://censusindia.gov.in/2011-common/censusdata2011.html>
- [5] <https://tis.nhai.gov.in/>
- [6] https://en.wikipedia.org/wiki/Transport_in_India